General Disclaimer

One or more of the Following Statements may affect this Document

- This document has been reproduced from the best copy furnished by the organizational source. It is being released in the interest of making available as much information as possible.

- This document may contain data, which exceeds the sheet parameters. It was furnished in this condition by the organizational source and is the best copy available.

- This document may contain tone-on-tone or color graphs, charts and/or pictures, which have been reproduced in black and white.

- This document is paginated as submitted by the original source.

- Portions of this document are not fully legible due to the historical nature of some of the material. However, it is the best reproduction available from the original submission.

LIMITS ON DIFFUSE X-RAY EMISSION FROM M101

D. McCAMMON and W. T. SANDERS
Physics Department, University of Wisconsin, Madison

ABSTRACT

Observed limits on diffuse X-ray emission from M101 require that the temperature of any coronal or matrix hot gas which is radiating an appreciable part ($\gtrsim 10\%$) of the average supernova power be less than $10^{5.7}$ K. Furthermore, the fraction of the galactic plane occupied by hot bubbles similar to the one which apparently surrounds the Sun is at most 25% in the region between 10 kpc and 20 kpc from the galactic center.

I. INTRODUCTION

The most straightforward interpretation of existing soft X-ray diffuse background data implies that the Sun is located within a region of approximately 100 pc radius which is filled largely with gas at about 10^6 K (Sanders et al. 1977; Tanaka and Bleeker 1977; Hayakawa et al. 1978; McCammon et al. 1983). It is of some interest to determine whether the Sun's location is fortuitous, or whether a large fraction of the galactic disk is similar to the local region, since the latter conclusion would have considerable impact on our conception of the general organization of the interstellar medium.

A second, possibly related, question pertains to the fate of the $\sim 10^{42}$ ergs s^{-1} average supernova input energy to the galaxy. Direct observation of X-ray emission from young supernova remnants such as the Cygnus Loop shows that some part of this energy goes into heating the ambient interstellar material to high temperatures. The existence of 10^6 K gas near the Sun and the ubiquitous presence of OVI in the galactic disk (Jenkins and Meloy 1974; Jenkins 1978a,b) suggest that this process may not be localized to the immediate vicinity of the supernova. In some models of the interaction of supernovae with interstellar material, the remnants can intersect and interact with each other before losing most of their energy to radiation, evaporation, or expansion. Such models generally result in a substantial fraction of the volume in the galactic disk being heated to $\sim 10^6$ K, and lead naturally to the formation of some sort of galactic corona, fountain, or wind which may radiate away much of the total supernova energy (Cox and Smith 1974; Chevalier and Oegerle 1979; Bregman 1980; Cox 1981; Habe, Ikeuchi, and Tanaka 1981). In at least one other view of the process,

mechanisms exist which allow the supernova remnants to dissipate their energy before they overlap (McKee and Ostriker 1977). The fraction of the galactic disk filled with hot, low density gas may still be large but the temperatures are lower and no corona or fountain is formed.

The major difficulty in any direct observational investigation of these possibilities is that it is necessary to determine the distribution of interstellar gas at temperatures near 10^6 K. Such material is easily detected only through its soft X-ray emission, and this, having a mean free path of only about 1×10^{20} H I cm^{-2}, cannot be observed in the galactic disk beyond the local low-density region. We have investigated other indicators, such as optical or UV forbidden lines from the hot gas or recombination lines from photoionized atoms in surrounding cool material, but none seems at all practical. A more promising technique would be to look for X-ray resonance lines of highly ionized heavy elements in absorption (York and Cowie 1983), but this will not be easy even with AXAF-class instrumentation.

Another approach is to look for evidence of hot gas in other normal galaxies. With the _Einstein_ observatory it is possible to make observations with the required high spatial resolution, and foreground extinction is not too serious if targets at high galactic latitude are chosen. Extended emission associated with elliptical galaxies has been observed for some apparently normal members of loose clusters (Forman et al. 1979; Canizares et al. 1979; Bechtold et al. 1983) and small groups (Biermann and Kronberg 1983) as well as for the active galaxies Cen A (Feigelson et al. 1981) and M82 (Watson et al. 1983). In most cases the emission is probably from diffuse hot gas, but the origin of the hot material is uncertain. While this is an interesting subject in its own right, we will limit the current

investigation to spiral galaxies, since the nature of the interstellar medium in ellipticals is clearly quite different.

Observations of edge-on spirals provide extremely high sensitivity to emission from galactic coronae or fountains which extend above all of the neutral gas due to the long line of sight through the hot material. Bregman and Glassgold (1982) have used observations of two such galaxies to eliminate the possibility that a large fraction of the supernova energy is being radiated by a corona at any temperature between $10^{5.6}$ K and $10^{7.0}$ K. Observations of face-on spiral galaxies are somewhat less sensitive to coronae, but emission limits would not depend critically on the assumed z-distribution of the emitting and absorbing material, and it would be possible to see hot gas within the galactic disk of the face-on spiral.

After selecting possible targets for foreground column density less than 2×10^{20} H I cm^{-2}, inclination angle less than 30°, angular diameter between 12′ and 30′, and existing IPC observations of more than 10,000 s, we are left with only one candidate which is a reasonably normal spiral. This is M101, a type Sc supergiant (Van den Bergh 1960) which is almost perfectly face on, has a Holmberg radius of 14′ (Allen et al. 1978), and a foreground column density of 1.1×10^{20} H I cm^{-2} (Heiles and Stark 1983). Two IPC observations of M101 were made as part of Columbia University's survey of normal galaxies: a 12,000 s exposure on 1979 January 6 and a 7,000 s exposure on 1979 May 16. An analysis of the discrete sources in these images has been presented by Long and Van Speybroeck (1983).

II. DATA REDUCTION

Analysis of IPC data for diffuse sources is complicated by several factors. These include a rather high and sometimes variable non-X-ray background, large gain variations with position on the detector, gain variations with time, vignetting, shadowing by the window support ribs, and contributions from poorly-resolved point sources. The non-X-ray background is particularly serious since it has a strong energy dependence which combines with the local gain variations to produce apparent spatial structure when a finite pulse height range is selected from uncorrected data.

Due to the efforts of the _Einstein_ staff at the Center for Astrophysics, these problems are now fairly well understood, and corrections can be made. The tests described in §III indicate that the corrections are reasonably successful, and that the data can be used for the purpose of this paper with some confidence. The procedure used consists of the following steps, several of which are included in the current IPC image reprocessing project:

1. Count rate integrated over the IPC field is plotted as a function of time for various groups of pulse-height channels. Times when the count rate rises above the observed minimum by a significant amount (5%-15%) are removed from the observation.

2. Position-dependent gain variations are removed with the aid of the Diffuse Gain Normalization Image (DGNI). This image is the product of a long preflight exposure of the IPC to an aluminum Kα X-ray calibration source, and gives the mean pulse height (BAL) observed at each position on the detector. Given the correct BAL, a standard subroutine uses preflight

nonlinearity calibration data to determine the actual energies of the pulse height channel boundaries. For each X-ray event in the image being analyzed, the gain at its position (the local BAL) is looked up in the DGNI file and the energy boundaries of the pulse height bins are calculated for both the local BAL value and for a standard BAL of 16.0 to which the entire image is being reduced. The count is assumed to be uniformly distributed across the energy range of the bin in which it occurs at the local BAL value, and it is divided up proportionally among the one or more output (BAL=16.0) bins which overlap it. This is equivalent to a Monte Carlo approach to assigning an output bin for the count when more than one output bin overlaps the input bin. Sort-file data are used since the 32-channel pulse height information available there minimizes smearing introduced by the bin shifting. IPC channels referred to elsewhere in this paper are the standard 16 channels used in the image files. Since the DGNI data were taken at an IPC gain giving an average BAL value of 15.8, while the images used in the analysis have average BALs ranging from 13 to 18, we had to scale the DGNI data to our actual average BALs. To do this we assumed that the ratio of local aluminum Kα mean pulse heights at different points on the detector would be independent of gain. This is unrealistic because gain saturation nonlinearity will compress the ratios at higher gains and expand them at lower gains. Over the limited range of image BAL values encountered here, however, we do not expect this to be a major effect. In cases where the gain changed significantly during an exposure, the image was broken up into several time segments, and an appropriate gain value was used in correcting each segment.

3. Vignetting corrections have been determined from observations of fluorescence and scattering from the Earth's atmosphere when it is illuminated by the Sun, A combination of these "flat field" data, preflight measurements, and calculated values have been used to prepare the vignetting tables used at the Center for Astrophysics. For the lower energies of interest here, the corrections are almost independent of energy, and the different determinations are in good agreement.

4. Discrete sources in the field are identified by visual inspection of contours on a spatially smoothed version of the corrected data and by comparison with sources identified during the original production processing of the images. Circular areas centered on the source locations are eliminated from consideration when calculating the diffuse surface brightness. The excluded diameters range from 30 pixels (4') for the fainter sources up to 60 pixels (8') for the brightest.

5. A region extending for 30 pixels on either side of the window support rib centers was also excluded, as was all area within 30 pixels of the edge of the field of view. These large zones of avoidance were necessary due to the poorer spatial resolution of the IPC at small pulse heights.

6. Counts outside of these excluded areas were added for a series of 5' annuli surrounding the center of M101. Figure 1 shows these annuli and the excluded areas superimposed on an image of M101 taken from the PSS red print. Adopting a distance of 7.2 Mpc for M101 (Sandage and Tammann 1974; Allen et al. 1978) gives a scale of about 2 kpc/arcmin. The Holmberg diameter is 28' (Allen et al. 1978).

7. Steps 1-6 are repeated for a long IPC exposure taken with a thin aluminum filter in front of the detector. The filter blocks most of the X-rays, but since it is quite thin it has little effect on most of the sources of non-X-ray background. The residual contribution from that part of the diffuse X-ray background transmitted by the filter was estimated by using the diffuse X-ray data from the Wisconsin sky survey (McCammon et al. 1983) in an 8° field surrounding the pointing direction of the filter image. An $E^{-1.4}$ power law plus two-temperature optically thin thermal bremsstrahlung spectrum (Raymond and Smith 1979) was fit to the sky survey data and the predicted response of the filter/IPC combination to this spectrum was subtracted from the filter image rates. This correction was quite small at the low energies of primary interest here. The vignetting corrections are of course meaningless when applied to non-X-ray background, but since identical corrections have been applied to the non-X-ray background portion of the primary image they do not affect the background subtraction process of step 9.

8. If the guard counter rate for the primary image is significantly different from that for the filter image, the observed non-X-ray rates in the filter image are corrected for this difference using slopes of IPC rate vs. guard rate plots compiled by D. Fabricant (1982). Where these data are available only for pairs of channels, the counts are arbitrarily assigned half to each channel. In all cases this correction is small.

9. The corrected filter image is scaled to the net exposure time of the primary image and subtracted from it. Rates in each of the concentric rings are divided by the net area of the ring after exclusions to give surface brightness rates in counts s^{-1} arcmin^{-2}.

The second IPC observation of M101 had relatively large fluctuations in total counting rate during each orbit, with little time spent at a low-rate plateau. Since this exposure started out with only 7,000 seconds, the small useable fraction would add little to the statistical accuracy of the overall results, and only the first observation was included in this analysis.

III. TESTS OF CORRECTION PROCEDURES

We have made two kinds of tests of the correction procedures described above. The first is an "empty field" test on a long exposure taken in the galactic plane. This image contains only a few faint discrete sources, and it is in a region where the Wisconsin sky survey shows no large-scale structure in the diffuse background. The image was corrected using the same procedures used for the M101 image, and the net X-ray rates for each of the concentric rings are given in Table 1. The average rates in each of these rings for the M101 image are given for comparison. Uncertainties given are purely statistical. The small variations with radius which remain in the empty field image may be due to limitations in the accuracy of the vignetting corrections and residual detector nonuniformities which were not removed by the correction procedures, or they may be indicative of real small-scale structure in the diffuse X-ray background.

The corrected rates observed in the outermost rings of the M101 image, where there should be no emission associated with that galaxy, and in all of the empty field image are presumably due to the diffuse X-ray background. We would gain a great deal of confidence in our non-X-ray background subtraction and correction procedures if these spectra can be shown to agree with independent measurements of the diffuse background.

Observed rates in all seven energy bands of the Wisconsin sky survey in $8°$ fields centered on the IPC image locations were fit with power-law plus two-temperature thermal bremsstrahlung (Raymond and Smith 1979). The equilibrium thermal emission models probably are not realistic, but all spectra which satisfy the constraints of the multi-band sky survey data will certainly produce identical responses in the IPC, which has lower energy resolution and a smaller bandwidth. The computed responses of the IPC to these spectra are shown in Figure 2 along with the corrected IPC data. We emphasize that there are no free parameters in the predicted pulse height spectra.

The diffuse X-ray background differs in absolute intensity by about a factor of two between the two locations, and has a noticeably different spectrum. In both cases the corrected IPC spectra still agree to 25% or so with predictions based on the sounding rocket observations. This discrepancy is somewhat larger than the statistical uncertainties in the sky survey data averaged over these small areas, but there is no way to rule out spatial fluctuations on scales smaller than the $8°$ survey resolution. It does appear that the predictions may be systematically high at the lower energies, which would indicate uncertainties of this magnitude in modelling the IPC response to very low-energy X-rays.

As a test of sensitivity to gain parameters, we reanalyzed the data assuming average gain (BAL) values 1.0 higher and lower than the nominal calibration. Actual gain uncertainties should be well within these limits, and the effects were in all cases comparable to or less than the one sigma statistical errors.

These results are by no means ideal. Given the large background, gain, and vignetting corrections, however, they are about as good as could be expected, and they lend confidence at least to rough quantitative conclusions drawn from diffuse emission observations with the IPC.

IV. DISCUSSION

Figure 3 shows contours of the smoothed count rate distributions in the M101 IPC field for two pulse height ranges. Most of the very luminous binary X-ray sources emit strongly in the 0.8-3.5 keV range shown in Figure 3a, while diffuse thermal emission such as that observed in our own galaxy shows up most strongly in the 0.17-1.5 keV band used in Figure 3b.

A number of discrete sources can be seen in the high energy range, and most of those in the central part of the field are probably associated with M101. If these are individual sources, they must be considerably more luminous than any in our galaxy (Long and Van Speybroeck 1983). In the low energy range, a quite different set of sources appears prominent. The ones near the edges of the field are probably foreground stars, but the bright, obviously extended source is well-centered on the optical image of M101 and is surely associated with it.

Since the energy range is right for diffuse thermal emission and the intensity distribution is clearly inconsistent with a single point source, it is tempting to ascribe this feature to just the sort of diffuse emission we might have expected. Some caution is in order here, however: Since the spatial resolution of the IPC is poorer for these low pulse heights, as few as three discrete sources could reproduce most of the observed intensity distribution. That a few sources do, in fact, contribute a substantial

fraction of the observed flux is demonstrated by time variability. In a shorter exposure made about six months after this observation, the peak of the distribution has moved 2′ to the east, and is then coincident with one of the sources visible in the channels 6-12 map. This source has increased in brightness by about 50% at the higher energies over the same time interval. Meanwhile, the low-energy intensity at the former position of the peak has dropped more than a factor of two.

The total energy in the feature is about 10^{40} ergs s^{-1} (assuming D=7.2 Mpc). A substantial fraction of this must be due to discrete sources, and all of it could be, but since there is no way to determine the point source contribution, we will simply treat it as an upper limit to the diffuse emission. In this context it should be noted that the areas surrounding high energy discrete sources which have been excluded from the analysis fortuitously exclude the brighter portions of this low-energy distribution. As an estimate of the possible effects of this, the two-sigma upper limit to the channels 2-4 flux excess in the central 5′ circle as compared to the outermost rings increases by a factor of 1.3 if no area is excluded from the central circle.

To find an upper limit to the total diffuse luminosity of M101, we have used the equilibrium thermal emission models of Raymond and Smith (1979). It may not be reasonable to expect thermal equilibrium in most scenarios of diffuse emission, but these spectra are a convenient standard, and we hope more detailed non-equilibrium calculations can be related to them.

For each assumed emission temperature, an optimum set of pulse height channels is determined by assigning a weight to each channel equal to the ratio of predicted rate to the square of the statistical uncertainty in the

observed rate. The average rate in rings 4 and 5 (15´-25´ radius) is assumed to represent the foreground and background diffuse emission, and is subtracted from the average rate over the central three rings. The third ring extends to just beyond the Holmberg radius, which is equal to 14´ (Allen et al. 1978). The emission measure of the model is then increased until the predicted rate is equal to the two-sigma upper limit on the observed excess rate in the central 15´. This emission measure can be converted to an upper limit on surface brightness by integrating the model over all energies (actually 10 eV to 5 keV).

The results of these calculations are shown in Figure 4. The parameter on the curves is the column density of cooler absorbing gas within M101 which is assumed to overlie the emitting material. Foreground absorption due to the $1.1{\times}10^{20}$ H I cm^{-2} along this line of sight in our galaxy is taken into account in all cases. Since the average total thickness of the neutral hydrogen in M101 is $6{\times}10^{20}$ H I cm^{-2} (Solomon et al. 1983), $3{\times}10^{20}$ seems to be a reasonable upper limit to the average overburden. For hot gas in the solar neighborhood, the effective column density to outside our galaxy averaged over $|b|{>}60°$ is slightly more than $1{\times}10^{20}$ H I cm^{-2}.

The dashed line shows the surface brightness corresponding to a total luminosity into 4π of 10^{42} ergs s^{-1} (one 10^{51} erg supernova per 30 years), assuming a distance of 7.2 Mpc. No interesting limits are placed for temperatures lower than $10^{5.6}$ K, since the fraction of the total energy radiated at wavelengths to which the IPC is sensitive becomes too small. For temperatures greater than ${\sim}10^7$ K, the emitting material would probably form a wind which would dissipate it over an area much larger than the galactic disk before it cooled (Bregman and Glassgold 1982). It seems

unlikely that a large fraction of the supernova power escapes at these high temperatures, however, since the very small limits at somewhat lower temperatures would require that the hot gas escape very efficiently, with less than 1% of its energy degraded to lower temperatures. Thus our limits on the temperature ranges over which the average supernova power could be radiated are quite similar to those obtained by Bregman and Glassgold (1982) using observations of edge-on spirals. The difference is that the limits for M101 do not depend on an assumption that the emission scale height is much larger than that for the absorbing material.

Another way of looking at limits on diffuse emission is to ask what fraction of the galactic disk might be occupied by hot regions similar to the one which seems to surround the Sun. To answer this we averaged the diffuse emission seen on the Wisconsin sky survey for $b > +60°$ and for $b < -60°$. The calculated contribution from an extragalactic 11 $E^{-1.4}$ photons cm^{-2} s^{-1} sr^{-1} component was subtracted from each of these, and the residual spectra were fitted with three-temperature Raymond and Smith (1979) thermal emission models. We assumed that all of this emission was entirely unabsorbed. This gives a lower limit to the derived galactic emission measure, since if part of the emission comes from beyond a portion of the absorbing gas layer, then a higher emission measure would be required to fit the observed flux and the galaxy would appear much brighter from the outside. The emission measures for the north and south polar regions were added to get the total emission measure through the local bubble.

These temperature fits are by no means unique, but all sets of temperatures and emission measures which gave an adequate fit to the Wisconsin sky survey data resulted in identical predictions for the IPC

counting rates. The temperatures and emission measures actually used here are shown in Table 2. With this model spectrum, the same procedure as described above was used to place upper limits on the fraction of the area of the disk of M101 which could have such emission measures.

Figure 5 shows the results of these calculations for areas at various distances from the center of M101. (Rings 4 and 5 were always used to determine the background rate.) Again, 3×10^{20} H I cm^{-2} seems a reasonable upper limit to the expected overburden of absorbing material, since this is half the average total gas thickness. If we wish to extend the analogy with the hot bubble around the Sun to the amount of overlying gas, then 1.3×10^{20} H I cm^{-2} is the appropriate number to use. For the central 5´, the observed intensity is roughly consistent with 100% of the area having the same emission measure as our local bubble. However, beyond 5´ the surface brightness limits drop rapidly, and for the area between 5´ and 10´ from the center (~10-20 kpc at 7.2 Mpc) no more than 24% of the area could have such an emission measure if it were overlaid by 1.3×10^{20} H I cm^{-2} or less.

V. CONCLUSIONS

Using a long Einstein IPC exposure of M101, we conclude that if the average supernova power in that galaxy is $\sim 10^{42}$ ergs s^{-1}, less than half can be radiated by hot gas at any temperature greater than $10^{5.8}$ K even if the hot material is overlaid by most of the neutral interstellar gas. This upper limit becomes less than 10% for temperatures greater than $10^{6.0}$ K, and less than 1% for temperatures greater than $10^{6.5}$ K. We also find that if all of the observed flux from within 5´ of the center of M101 were attributed to diffuse emission, it would be roughly consistent with ~100% of

that area being covered with hot bubbles similar to the one surrounding the Sun. The allowed fraction is much lower beyond 5˝, and at most 14% to 35% of the area between 5˝ and 10˝ from the center could be occupied by such objects, depending on the amount of absorbing material assumed to overlie them.

While these data should provide some useful constraints for general models of the interstellar medium and disposition of supernova energy in galaxies, it is clear that improved sensitivity and extension to a larger statistical sample would be highly desirable. A few more IPC images of galaxies are available which would be suitable for such analysis, but the one used here is probably by far the highest quality. On the other hand, currently planned facilities (ROSAT and AXAF) will offer greatly improved sensitivity for this type of observation, plus better spatial resolution which should allow removal of discrete source contributions to a much lower level. It therefore seems likely that observations of other galaxies will provide a great deal of information on the nature of this hot phase of the interstellar medium which is so difficult to observe in our own.

Reduction and Analysis Facility (MADRAF) were used for image analysis. This work was supported in part by NASA grant NAG 8-431.

TABLE 1

X-Ray Count Rates[a] in Concentric Rings

Ring	Radius		Empty Field $\ell=57^\circ\!.0$, $b=0^\circ\!.0$ (10^{-4} counts s^{-1} arcmin^{-2})	M101 Field $\ell=102^\circ\!.0$, $b=+59^\circ\!.8$ (10^{-4} counts s^{-1} arcmin^{-2})
	From	To		
1	0' – 5'		2.10 ± 0.15	5.30 ± 0.67
2	5' – 10'		2.01 ± 0.08	3.86 ± 0.19
3	10' – 15'		1.99 ± 0.07	3.53 ± 0.13
4	15' – 20'		1.89 ± 0.09	3.88 ± 0.16
5	20' – 25'		1.77 ± 0.17	3.72 ± 0.30

[a] Summed over pulse height channels 2-7.

TABLE 2

Adopted Emission Measures for Solar Neighborhood Hot "Bubble"

Temperature (K)	Emission Measure (cm^{-6} pc)
$10^{5.8}$	0.00319
$10^{6.2}$	0.00216
$10^{6.4}$	0.00372

REFERENCES

Allen, R. J., van der Hulst, J. M., Goss, W. M., and Huchtmeier, W. 1978, Astr. Ap., 64, 359.

Bechtold, J., Forman, W., Giacconi, R., Jones, C., Schwarz, J., Tucker, W., and Van Speybroeck, L. 1983, Ap. J., 265, 26.

Biermann, P., and Kronberg, P. P. 1983, Ap. J. (Letters), 268, L69.

Bregman, J. N. 1980, Ap. J., 237, 681.

Bregman, J. N., and Glassgold, A. E. 1982, Ap. J., 263, 564.

Canizares, C. R., Clark, G. W., Markert, T. H., Berg, C., Smedira, M., Bardas, D., Schnopper, H., and Kalata, K. 1979, Ap. J. (Letters), 234, L33.

Chevalier, R. A., and Oegerle, W. R. 1979, Ap. J., 227, 398.

Cox, D. P. 1981, Ap. J., 245, 534.

Cox, D. P., and Smith, B. W. 1974, Ap. J. (Letters), 189, L105.

Fabricant, D. G. 1982, Center for Astrophysics internal report.

Feigelson, E. D., Schrier, E. J., Delvaille, J. P., Giacconi, R., Grindlay, J. E., and Lightman, A. P. 1981, Ap. J., 251, 31.

Forman, W., Schwarz, J., Jones, C., Liller, W., and Fabian, A. C. 1979, Ap. J. (Letters), 234, L27.

Habe, A., Ikeuchi, S., and Tanaka, Y. D. 1981, Publ. Astr. Soc. Japan, 33, 23.

Hayakawa, S., Kato, T., Nagase, F., Yamashita, K., and Tanaka, Y. 1978, Astr. Ap., 62, 21.

Heiles, C., and Stark, A. A. 1983, private communication.

Israel, F. P., Goss, W. M., and Allen, R. J. 1975, Astr. Ap., 40, 421.

Jenkins, E. B. 1978a, Ap. J., 219, 845.

————. 1978b, Ap. J., 220, 107.

Jenkins, E. B., and Meloy, D. A. 1974, Ap. J. (Letters), 193, L121.

Long, K. S., and Van Speybroeck, L. P. 1983, in Accretion Driven Stellar

X-ray Sources, ed. W. H. G. Lewin and E. P. J. van den Heuvel

(Cambridge: Cambridge Univ. Press), in press.

McCammon, D., Burrows, D. N., Sanders, W. T., and Kraushaar, W. L. 1983,

Ap. J., 269, 107.

McKee, C. F., and Ostriker, J. P. 1977, Ap. J., 218, 148.

Raymond, J. C., and Smith, B. W. 1977, Ap. J. Suppl., 35, 419.

————. 1979, private communication (update to Raymond and Smith (1977)).

Sandage, A., and Tammann, G. A. 1974, Ap. J., 194, 223.

Sanders, W. T., Kraushaar, W. L., Nousek, J. A., and Fried, P. M. 1977,

Ap. J. (Letters), 217, L87.

Solomon, P. M., Barrett, J., Sanders, D. B., and de Zafra, R. 1983,

Ap. J. (Letters), 266, L103.

Tanaka, Y., and Bleeker, J. A. M. 1977, Space Science Reviews, 20, 815.

Van den Bergh, S. 1960, Publ. David Dunlap Obs., 2, 157.

Watson, M. G., Stanger, V., and Griffiths, R. E. 1983, Ap. J., submitted.

York, D. G., and Cowie, L. L. 1983, Ap. J., 264, 49.

FIGURE CAPTIONS

FIG. 1.--Optical image of M101 from the Palomar Sky Survey red print. The 5″, 10″, 15″, 20″, and 25″ radius circles define the annuli used in analyzing diffuse emission. The smaller circular areas surround identifiable discrete sources and were excluded from the analysis, as were the rectangular areas surrounding the window support ribs. Crosses mark the locations of the three historical supernovae in M101 (Israel, Goss, and Allen 1975). The x at the center of the concentric circles is at α (1950) = $14^h01^m30^s$, δ = $+54° 36′ 00″$.

FIG. 2.--(a) Data points are the observed net X-ray rate in the outer rings of the IPC image centered on M101. The solid line is the predicted IPC response to the average diffuse background spectrum observed in an 8° field from the Wisconsin sky survey (McCammon et al. 1983) which surrounds the IPC image. The dashed line shows the level of non-X-ray background which has been subtracted from the IPC data. (b) As in (a), but for an "empty field" IPC image centered at ℓ = 57°, b = 0°, where the diffuse background observed in the Wisconsin sky survey is about a factor of two smaller than at the high-latitude position of M101 and has a harder spectrum.

FIG. 3.--Contours of net X-ray surface brightness in the IPC image of M101. All corrections described in the text have been applied, but no image areas have been excluded. (a) PHA channels 6-12 (~0.8-3.6 keV), smoothed with a 2.1″ FWHM gaussian. Contour levels are 5, 8, 11, 14, and 17 × 10^{-4} counts s^{-1} arcmin^{-2}. (b) PHA channels 2-4 (~0.17-1.5 kev), smoothed with a 3.7″

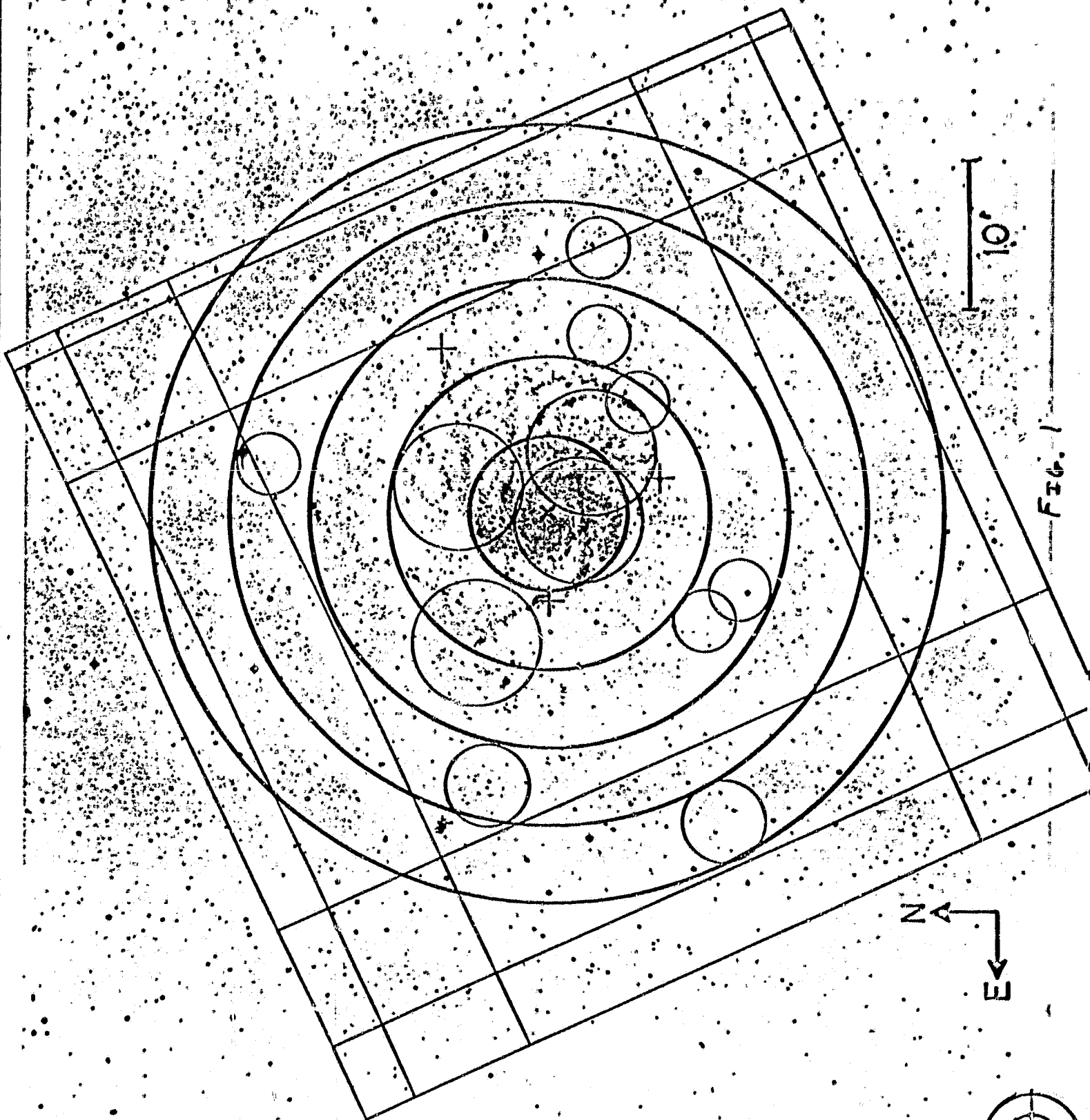FWHM gaussian. Contour levels are 5, 6, 7, and 8×10^{-4} counts s^{-1} arcmin^{-2}.

FIG. 4.--Two-sigma upper limits to total emission from hot gas as a function of temperature, averaged over the central 15" radius (the Holmberg radius is 14"). Assumed spectra are those of Raymond and Smith (1979). Limits on total energy are low at the higher temperatures, where a large fraction of the energy is emitted at wavelengths to which the IPC is sensitive. The parameter on the curves is the column density of cool gas within M101 that is assumed to overlie the emitting material. The dashed line shows the average surface brightness expected if 10^{42} ergs s^{-1} were being radiated by gas within the central 30 kpc (15" for an assumed distance of 7.2 Mpc).

FIG. 5.--Two-sigma upper limits to the fraction of the area in the disk of M101 which could be occupied by hot "bubbles" similar to the one which apparently surrounds the Sun as a function of the column density of cool absorbing gas which is assumed to overlie the bubbles. The parameter on the curves is the range of distances from the center of M101 to which the limit applies.

D. McCAMMON, and W. T. SANDERS:

Department of Physics, University of Wisconsin, Madison, WI 53706

FIG. 1

(a)

FIG. 2a

Fig. 2b

Fig. 3a

N

(b)

Fig. 3b

FIG. 4

FIG. 5